Scanning Microscopy

Volume 7 | Number 1 Article 6

1-21-1993

Quantitative Scanning Electron Acoustic Microscopy of Silicon

M. Domnik
Universität Duisburg

L. J. Balk
Universität Duisburg

Follow this and additional works at: https://digitalcommons.usu.edu/microscopy

Part of the Biology Commons

Recommended Citation

Domnik, M. and Balk, L. J. (1993) "Quantitative Scanning Electron Acoustic Microscopy of Silicon," *Scanning Microscopy*: Vol. 7 : No. 1 , Article 6.
Available at: https://digitalcommons.usu.edu/microscopy/vol7/iss1/6

This Article is brought to you for free and open access by the Western Dairy Center at DigitalCommons@USU. It has been accepted for inclusion in Scanning Microscopy by an authorized administrator of DigitalCommons@USU. For more information, please contact digitalcommons@usu.edu.

Scanning Microscopy, Vol. 7, No. 1, 1993 (Pages 37-48) 0891-7035/93$5.00+.00
Scanning Microscopy International, Chicago (AMF O'Hare), IL 60666 USA

QUANTITATIVE SCANNING ELECTRON ACOUSTIC MICROSCOPY OF SILICON

M. Domnik and L.J. Balk*

Universität Duisburg, Fachgebiet Werkstoffe der Elektrotechnik
Sonderforschungsbereich 254, Kommandantenstr. 60, W-4100 Duisburg 1, F.R.G.

Present address:
Bergische Universität Wuppertal, Lehrstuhl für Elektronik
Fuhlrottstraße 10, W-5600 Wuppertal 1, F.R.G.

(Received for publication May 10, 1992, and in revised form January 21, 1993)

Abstract

So far results of scanning electron acoustic microscopy (SEAM) have retained a widely qualitative meaning only due to the enormous uncertainty in understanding sound generation and contrast mechanisms in SEAM micrographs. In this work, a detailed treatment of these mechanisms has been undertaken for silicon resulting in precise knowledge of the signal generation processes and a well understood interpretation of the contrast mechanisms involved in imaging thermo-mechanical and electronic features.

Key Words: Scanning electron acoustic, microscopy, thermal waves, silicon, signal generation, metallizations, grain boundaries, doping contrast.

*Address for correspondence:
L. J. Balk
Bergische Universität Gesamthochschule Wuppertal
Lehrstuhl für Elektronik
Fuhlrottstraße 10, W-5600 Wuppertal 1
F.R.G. Phone No. (+49-202) 439-2972

Introduction

Since its introduction by Brandis and Rosencwaig [2] and by Cargill III [3] the method of scanning electron acoustic microscopy (SEAM) has demonstrated up to now its ability of imaging many material parameters and microscopic features. In this manner it has been applied to the investigation of silicon materials and devices. Examples in this sense are detection of selectively doped regions, grains and grain boundary properties in polycrystal-line silicon, crystalline defects and thermoelastic properties. However, even when restricting the SEAM method to the so-called linear mode, which utilizes harmonic primary beam amplitude modulation and detection of the generated sound signal at this modulation frequency f, the interpretation of the contrasts has at best been only qualitative and at worse ambiguous. There are many reasons responsible for this situation: The generation mechanism for acoustic waves due to electron impact can be understood via different theories, the most important ones are White's theory using a thermo-elastic model [9] and the photostrictive model using the change of the deformation potential due to excess carrier production introduced by Stearns and Kino [8]. A sound judgement on the validity of one of these models could not be achieved, as the typical detection scheme, a piezoelectric transducer directly attached to the sample, does not allow unambiguous signal interpretation. The latter is mainly due to the unavoidable acoustic interaction between sample and transducer, nonlinear behaviour of the transducer itself, and the high chance for spurious signal pick up.

In two preliminary papers, the authors demonstrated in principle the validity of a thermo-elastic signal generation mechanism for the linear SEAM mode [4,5]. The aim of the present paper is to complete the results gained there and to provide a consistent treatment and proof of this model. Furthermore, it is demonstrated that the contrast seen in SEAM micrographs is not explained solely by the sound generation mechanism but also by the influence of the electronic properties of the sample.

In the second section of this paper, the sound detection technique based on a capacitive transducer is described [6], and its equivalence to the usual piezoelectric detection is shown. The advantages of this new transducer with respect to the quantification of SEAM results are explained. In the third section, the signal generation is investigated experimentally, and these results are successfully interpreted by means of a modified White-theory. To ensure that no other mechanisms and spurious signals may intrude on the results, all investigations related to the signal generation problem are carried out for homogeneously doped wafers. The contrast within micrographs is analyzed in the fourth section for

a number of typical discontinuities within silicon materials and devices, such as metallizations, grain boundaries, and selectively doped regions.

Comparison Between a Capacitive and a Piezoelectric Transducer

The principal structure of a capacitive transducer as used in this work is shown in Fig 1. The specimen is mounted on a ring shaped electrode, which is an additional electrical shield for the center detection electrode. The detection electrode itself is about 5 to 10 μm separated from the specimen surface. The advantages of this transducer compared to piezoelectric detection are as follows [6]:

- the frequency response of the magnitude of the surface displacement signal can be directly correlated to thermoelastic theory without the many acoustic resonances typically present when a piezoelectric transducer is tightly connected to the sample,
- there is no sequal dependence on the material properties of the sensor, especially when varying the sample temperature (the gap between detection electrode and sample is vacuum),
- the detection arrangement is usable over a very wide temperature range (80 K - 500 K),
- spurious signals can be eliminated by variation of the bias voltage for the detection electrode (switching off this bias voltage allows direct determination of the total amount of these signals, such as possible for instance by the generation of high frequency electron beam induced currents),
- there is a simple relationship between the acoustic mag nitude and phase of the detected electrical signal (implying a lock-in amplifier for signal identification and recovery).

In spite of these differences, it can be shown that the results obtained - at least for a fixed frequency - are most comparable for both types of detectors. This situation is important, as the judgement on the various theories of signal generation assumes that no differences are due to different detection schemes. For specimen thicknesses which are large compared to the thermal diffusion length of the sample under test one not only can find an equal sensitivity of the detectors [6], but also a very similar temperature response as indicated in Fig. 2. For the same sample, for identical electron beam parameters (30 keV, 1μA, 10 kHz modulation frequency), and for temperatures above 130 K no significant differences can be observed (the measurements are corrected for changes in the capacity of the detector arrangement due to a temperature dependent variation of its physical dimensions). For low temperatures, however, the magnitude signals differ, the reason being that the thermal diffusion length in silicon is strongly increasing when lowering the temperature below 100 K. Thus, the piezoelectric transducer will be heated periodically via the silicon sample, which causes an additional signal to the original SEAM magnitude. The phase signals do not show any significant differences (the different signs are only arbitrary and due to the polarity of the bias voltage for the detection electrode of the capacitive transducer). In Fig. 3 a micro-indentation in silicon is imaged with both detectors. The two SEAM micrographs show essentially the same features. From these results one can conclude that SEAM experiments are comparable no matter whether a capacitive or a piezoelectric transducer was used.

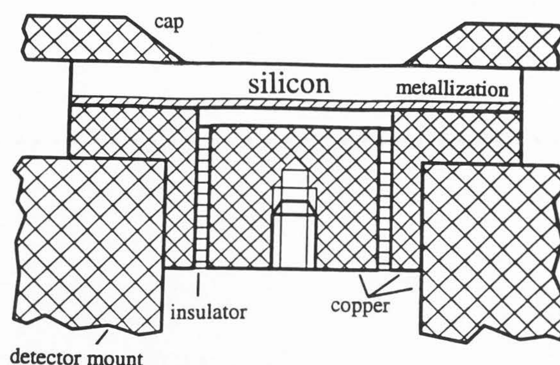

Figure 1. Schematic of capacitive transducer (the sample-electrode gap is formed by the distance of the metallization to the center copper electrode).

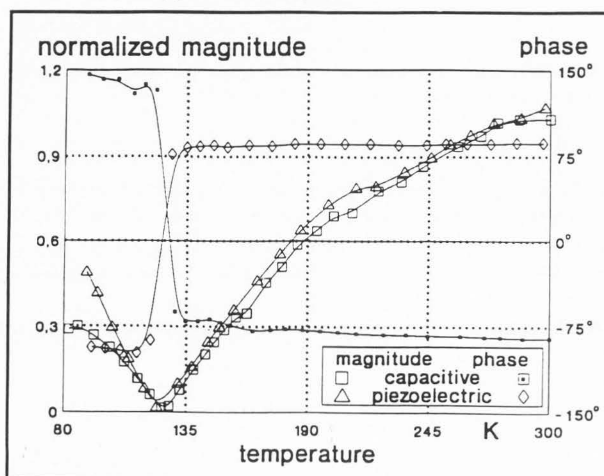

Figure 2. Temperature dependence of the electron acoustic signal for different detection techniques.

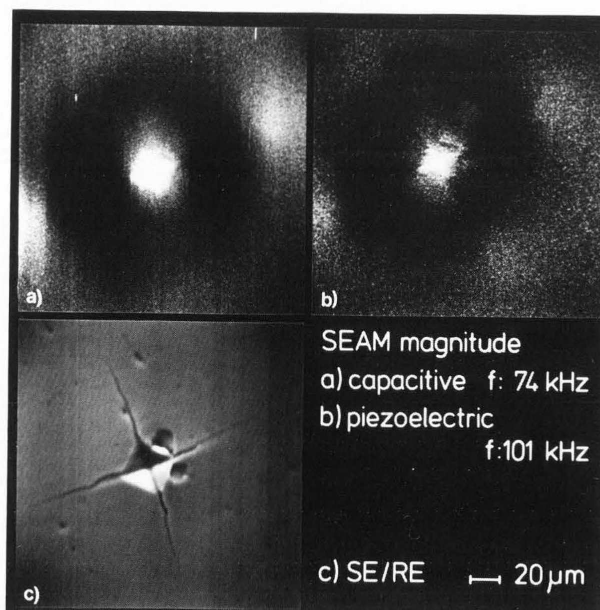

Figure 3. Indentation in silicon with piezoelectric and capacitive detection.
SE/RE: Secondary and reflected (backscattered) electrons.

This statement holds, furthermore, for the extension to photoacoustic experiments in which a laser is used for exciting the acoustic signal. Fig. 4 demonstrates the temperature dependence of the photoacoustic magnitude and phase as detected piezoelectrically. Again, the signal decays close to the temperature of 120 K (for which the linear thermal expansion coefficient α of silicon vanishes) consistent with White's treatment. Also at 120 K, the sign of the signal changes causing a 180°-step of the phase (due to the sign inversion of α at 120 K). However, looking closer, these features are less pronounced as for the SEAM results. Further reduction of temperature leads to a strong increase of the magnitude which considerably deviates from theoretical expectation (compare Fig. 5). As can be seen directly by Fig. 5, this is solely a consequence of a changed thermal situation. For temperatures below 100 K, the thermal diffusion length strongly exceeds the specimen thickness of, in this experiment, 525 µm. Thus, the signal increase in the low temperature range is due to thermal heating of the transducer. This supports the result of Fig. 4 which does not reveal anything else than thermo-elastic properties.

This issue was discussed here to emphasize:

a) the results obtained are comparable whether using capacitive or piezoelectric detection for either electron or laser beam excitation,
b) neglecting the thermal thickness of the sample for the piezoelectric transducer may lead to false conclusions concerning the temperature dependence of the signal magnitude.

In the following section, these two items are important when judging the validity of different models and experiments.

Signal Generation

To ensure that no extraneous signals may contaminate the detected signal, homogeneously doped silicon wafers have been used to determine the origin of SEAM signals. Three different influences on the SEAM signal should be mentioned:

a) the frequency behaviour will always be superimposed by acoustic resonances of the specimen and its housing (for both piezoelectric and capacitive detection),
b) the signal will tend to zero (for thermo-elastic coupling) when the linear expansion coefficient α vanishes (for silicon at about 120 K) and the SEAM phase will change when the sign of α changes,
c) the signal will show different frequency behaviour depending on the relationship of the thermal diffusion length λ_{th} to the specimen thickness d, i.e. a thermally thick sample ($\lambda_{th} < d$) behaves differently than a thermally thin one ($\lambda_{th} > d$).

On the Validity of Thermo-Elastic Signal Generation

To enable quantitative comparisons, all temperature dependent measurements were carried out under identical excitation conditions, especially for an arbitrarily chosen frequency of 10 kHz, which was in all cases well separated from any acoustic resonance. This arbitrary restriction, however, does not limit the validity of the results obtained. This is well demonstrated by Fig. 6 in which the SEAM frequency response is plotted for various temperatures. The phase change when passing 120 K is indicated here by artificial introduction of a polarity factor to the magnitude (positive is below 120 K, negative above it). Even at the position of strong resonance at 90 kHz the signal sign inversion, i.e. phase change = π, is clearly visible. The temperature behaviour shown in Fig. 6 can directly be explained by White's theory [5,9]. Furthermore, this sample undergoes a transition from a thermally thin to a thermally thick specimen causing a frequency independent magnitude at low temperatures (aside from the resonances) to a 1/f-magnitude law at high temperatures [5]. This causes a frequency dependent temperature behaviour of the SEAM magnitude. As can be seen by Fig. 7, the case of a thermally thin sample is reached at higher temperatures for 10 kHz (due to the change of the thermal diffusion length with $1/\sqrt{f}$) giving rise to an early saturation of the magnitude for decreasing temperatures (<90 K). For 55 kHz the signal can increase further due to the still existing 1/f-magnitude dependency for a thermally thick specimen. In any case, one can judge from Fig. 7 that for typical wafer material of about 500 µm thickness there will be always the case of a thermally thick sample at room temperature. Therefore all room temperature SEAM experiments for this type of sample must exhibit a 1/f-magnitude law for frequencies f ≥ 10 kHz, only overlayed by the resonances of the vibrating sample according to the theory by Rousset et al. [7]. This could already be proven for low doped material [5]. In Fig. 8, the same proof is given for a highly p-doped wafer. The

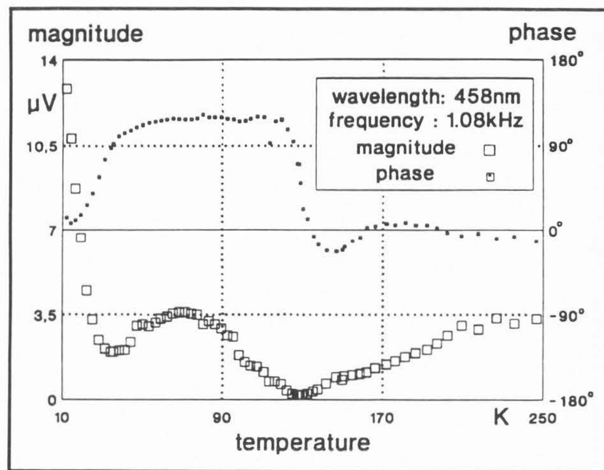

Figure 4. Temperature dependence of the photoacoustic signal in silicon.

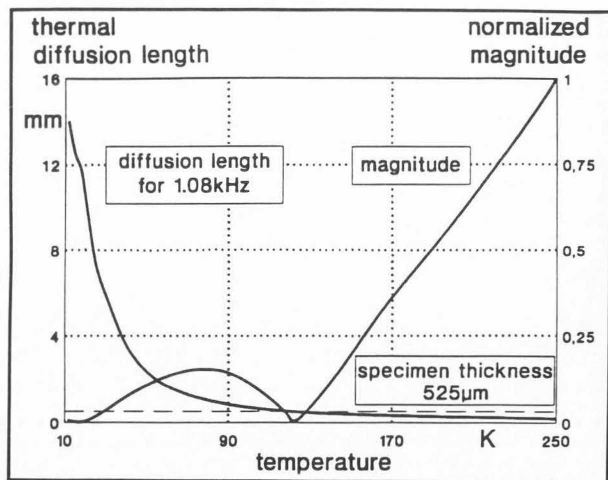

Figure 5. Calculated thermal diffusion length and normalized thermo-elastic magnitude in silicon.

consistency between experiment and theoretical calculation is obvious. To ensure the sole thermo-elastic origin of this signal dependency the same experiment was carried out for an aluminum sample in Fig. 9. Again, a nearly perfect match between experiment and the thermo-elastic theory is achieved. For Figs. 8 and 9, the calculation was carried out merely by considering the frequency dependence of the thermo-elastic sound generation and the resonant vibration of the sample at a frequency f_R with a damping factor δ:

$$A(f) \approx \frac{1}{f} \cdot \left[\left(f_R^{\,2} - f^2 \right)^2 + \delta^2 f^2 \right]^{-1/2}$$

Quantitative Determination of the Thermal Diffusion Constant

Describing the SEAM frequency dependence becomes more complicated than in the previous paragraph, if the thickness of the specimen is reduced thus leading to a transition from a thermally thick to thermally thin sample. According to Rousset et al. [7], the thermo-elastic magnitude becomes independent of frequency for a thermally thin sample. Such a transition may be achieved by variation of the sample temperature [5]. For a constant temperature, say for instance room temperature, the same effect may be obtained by a suitable choice of specimen thickness and frequency range. Now, due to the relation $\lambda_{th} = [D_{th}/\pi \cdot f]^{1/2}$,a determination of the transition temperature allows experimental evaluation of the thermal diffusion constant D_{th}. Following

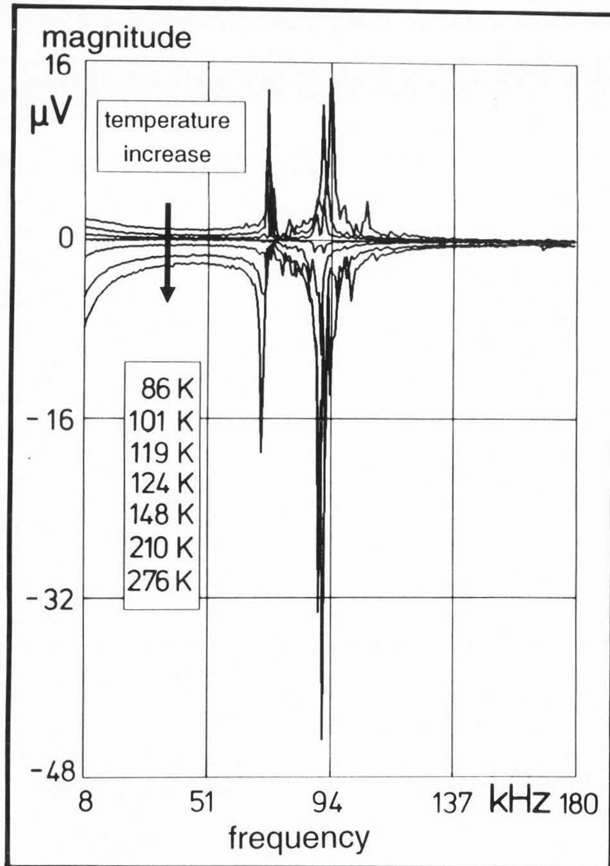

Figure 6. Temperature dependence of the electron acoustic signal in silicon.

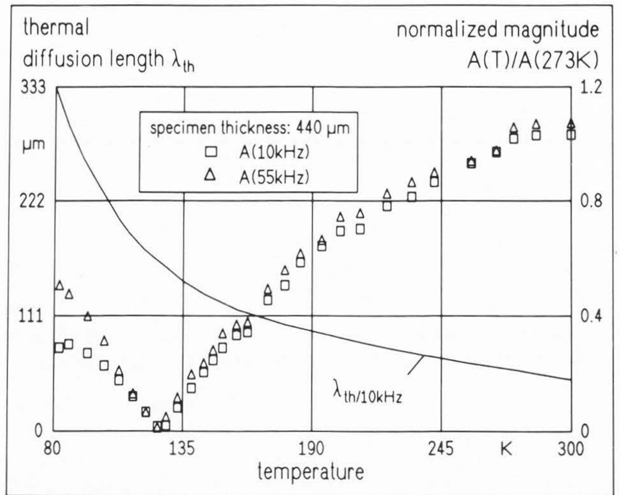

Figure 7. Different thermal status (λ_{th} > or <d) for different frequencies.

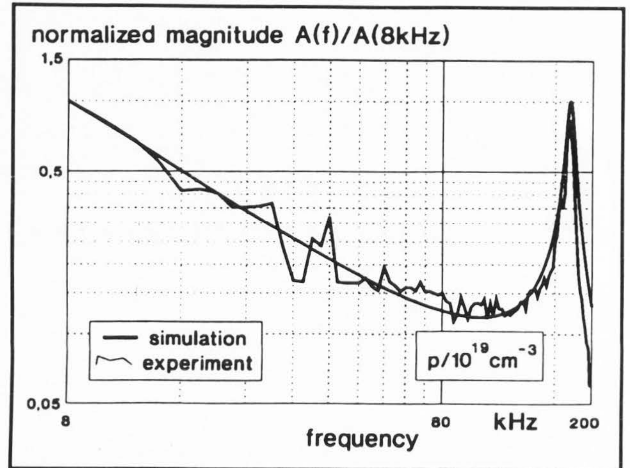

Figure 8. Calculated and measured normalized magnitude of boron doped silicon.

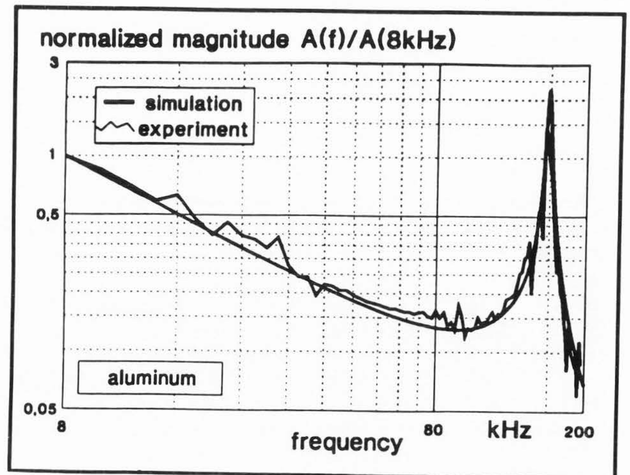

Figure 9. Frequency dependence of the electron acoustic magnitude in aluminium.

the treatment by Rousset et al. [7] the thermo-elastic frequency behaviour is to be described by hyperbolic functions of just one argument. This argument consists of the frequency f and of a single simulation parameter $\bar{a}$. $\bar{a}$ itself is a function of specimen thickness and the thermal diffusion constant D_{th}. Thus fitting the calculation to the experiment by optimizing $\bar{a}$ is equivalent to the determination of D_{th}.

This is demonstrated in Fig. 10 for a 195 μm thin sample. The transition from a frequency independent signal (for a thermally thin sample) to a frequency dependent magnitude at about 5 kHz is clearly visible. The low resonance frequency of ~ 40 kHz is due to the smaller specimen thickness. Two different simulations are shown, one (with $\bar{a}$ = 0,0167 $s^{1/2}$) is fitted to the low frequency regime, whereas the other one is fitted to the resonance region. As the first parameter fitted best in the transition range, this value was chosen to determine D_{th}. The value achieved for D_{th} is 1.6 cm^2/s, which is in reasonable agreement with the mean value in literature of about 1 cm^2/s. Additionally, one can see by Fig. 11 that the simulation fits the phase change as well as the magnitude. One should emphasize here that these experiments agree with theory in spite of a considerably different condition. The experiment used a finely focussed electron beam, whereas in theory a homogeneous illumination of the sample is assumed.

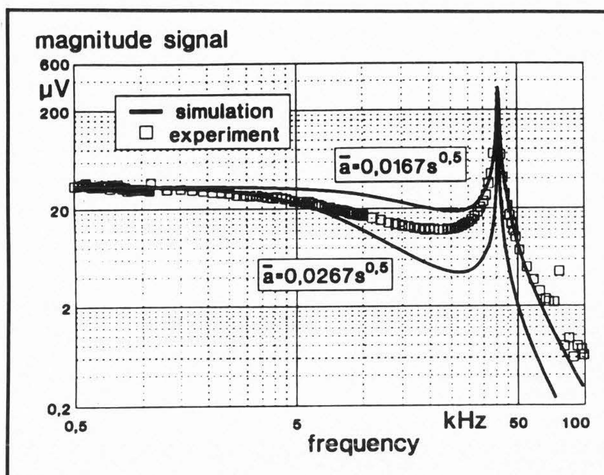

Figure 10. Transition effects on the electron acoustic magnitude for different thermal specimen thicknesses.

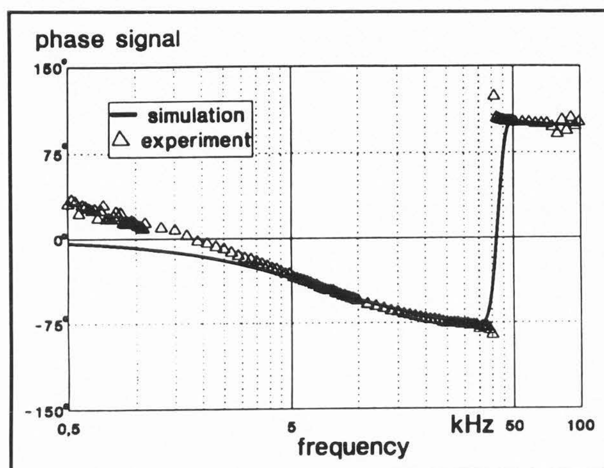

Figure 11. Transition effects on the electron acoustic phase for different thermal specimen thicknesses.

On the Influence of Specimen Preparation

To achieve a small specimen thickness, as necessary in the previous paragraph, commercially prepared silicon wafers have to be milled and polished. Such a mechanical treatment should suppress the photostrictive coupling between excess carriers and lattice according to Stearns and Kino [8]. However, all results as obtained in this work were independent of the mechanical and chemical surface treatment. This shall be demonstrated here for the example a three layer package consisting of an untreated silicon sample, a copper foil, and a heavily mechanically treated silicon. The untreated sample should definitely exhibit a photostrictive coupling due to Stearns and Kino resulting in a changed magnitude and, more strikingly, in a 180°-phase difference with respect to copper.

Across this Si-Cu-Si package, SEAM linescans were taken, with a primary electron energy of 30 keV a typical result being shown in Fig. 12. There is the expected material contrast visible for the magnitude between copper and silicon, but no significant contrast between the two types of surface preparations for the silicon samples. Merely strong defects like a bad adhesion between copper and silicon or a breaking within one of the silicon samples become evident. Even more important, the phase signal is in principle equal for all three samples. These two results clearly indicate that - at least for the kHz regime - a photostrictive effect cannot contribute significantly to the overall SEAM signal. Therefore, one can again conclude that the thermo-elastic signal generation is dominant in silicon.

Contrast Mechanisms

Contrast within SEAM micrographs of silicon materials and devices may be ambiguous, especially if the volume the contrast originates from is smaller than the thermal diffusion length λ_{th}. As λ_{th} may vary both due to temperature and to variation of the modulation frequency f, according variations of the contrast within the thermo-elastically generated signal can occur. Thus significantly different image appear-

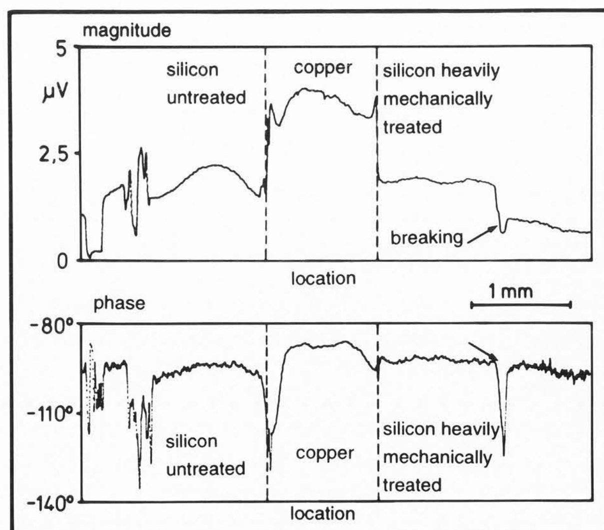

Figure 12. Effect of different preparation techniques on the electron acoustic signal.

ences may result from different experimental parameters but still be consistent with the thermo-elastic theory discussed above.

In the following, three typical contrast problems are discussed. The first example deals with the effect of an extrinsic layer on silicon in the form of a metallization, such as usually present on the surface of an integrated circuit. The two other examples are intrinsic effects within the silicon material, one a grain boundary, the other an ion implanted region.

Metallization Layers

The effect of a metallization on SEAM contrast was examined for a large number of very differently doped silicon wafers by the authors (from 3.5 mΩm to 10 kΩcm). All experiments showed the same results. Thickness of the layer and frequency were chosen to yield comparable relations between layer thickness and thermal diffusion length to the Stearns and Kino experiment [8]. The metallization was in all cases a 1 µm thick aluminum which was separated from the otherwise untreated silicon wafer by two intermediate layers of 200 nm TiN and 20 nm Si_3N_4. To clarify the above mentioned problem of the relation between the volume of contrast origin, here termed the information volume, and the thermal diffusion length, the primary electron energy was chosen to 10 keV assuring that all primary beam energy dissipation occurs within the metallization. This means complete absorption of the electron beam within the metal. Consequently the wafer itself is only heated indirectly by heat diffusion. To allow a precise evaluation of the resulting image contrast parts of the wafer surface were uncoated enabling the recording of SEAM signals of neighbouring locations, one metallized, the other untreated silicon. This kind of sample is denoted as partially metallized in the following.

Fig. 13 shows two frequency scans of magnitude and phase for these two positions. Though on first sight, these results seem to be identical, two important features can be recognized at once. The phase signal for Al and Si is always different, the magnitude signals are crossing each other. As this result of Fig. 13 is strongly disturbed by the resonances of the sample, it is quantified by the following two figures, Fig. 14 showing the magnitude contrast as the ratio of magnitude A on Al versus magnitude A on Si, and Fig. 15 exhibiting the phase contrast as the difference between the phases on Al and on Si. From Fig. 14 one can realize that independent of signal level and vibration status (resonant or non-resonant) the contrast rises monotonically with frequency. According to the crossing of the magnitude plots in Fig. 13 a vanishing of the contrast occurs at 60 kHz combined with a contrast inversion: below 60 kHz the aluminum would appear darker than silicon, above 60 kHz brighter. At 60 kHz, the metallization would yield no contrast at all. This behaviour is in perfect agreement with thermo-elastic theory:

The frequency behaviour of a thermally thin layer - as in this case - assumes that the thermo-elastic signal originates from a half-sphere of radius λ_{th} with $\lambda_{th} \sim f^{-1/2}$. Thus the volume v for signal origin follows the law $v \sim f^{-3/2}$. In contrast to this frequency dependent volume there is no change for the information volume, as this is determined mainly by the structure itself. Therefore the portion of the magnitude contrast K to the total signal must be proportional to 1/v. Following the previous definition of the contrast it follows that:

$$K(f) = s \cdot f^{3/2} + 1$$

with s as a scaling factor. With this formula the simulated curve of Fig. 14 was calculated. Similarly the phase contrast exhibits an unequivocal frequency dependence (Fig. 15). It

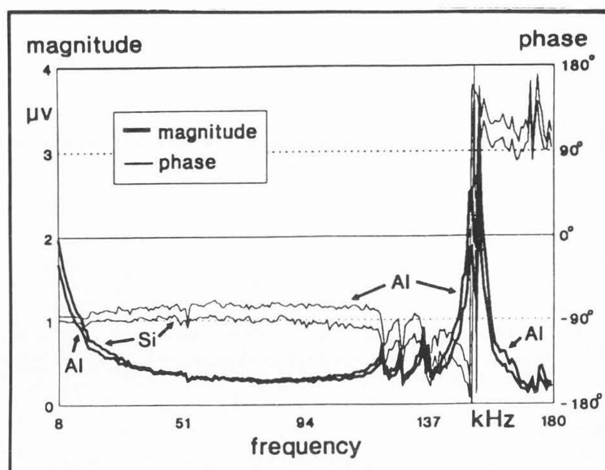

Figure 13. Frequency dependence of electron acoustic signals of a partially metallized surface.

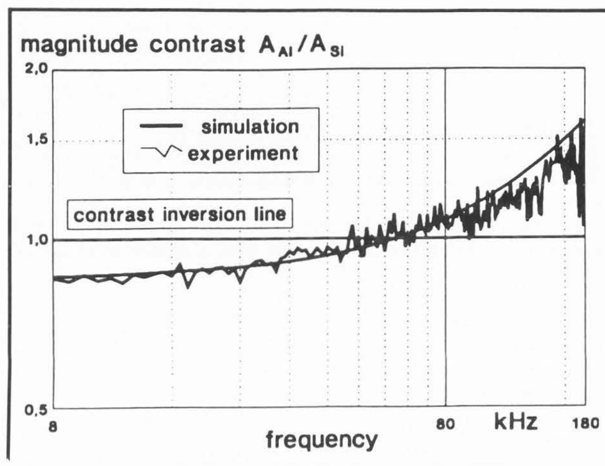

Figure 14. Calculated and measured magnitude contrast of partially metallized silicon.

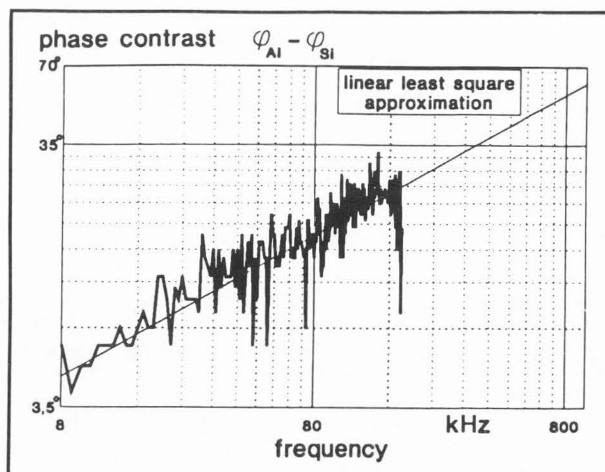

Figure 15. Electron acoustic phase contrast of partially metallized silicon.

demonstrates that the contrast increases with the reduction of λ_{th} and its approach towards the metallization thickness.

In the same manner as for frequency dependent experiments, the temperature behaviour of SEAM micrographs is affected by the relation between metallization thickness and thermal diffusion length. For uncoated silicon, a step-function-like 180° change of the SEAM phase occurs at 120 K which is strongly diminished for the metallization (Fig. 16). This reduction of phase change is different in size depending on the modulation frequency used. For higher frequencies, i.e. small thermal diffusion length, it may vanish since the whole signal arises from the metal layer itself. Parallel to the reduction of the observed phase change, a deviation from the zero level at 120 K within the magnitude signal becomes obvious at the metallized location (Fig. 17). The plot for the metallic surface has a minimum value shifted along the temperature scale with respect to the zero level of the uncoated surface; and again a crossover occurs between the magnitude signals of Al and Si with a subsequent contrast inversion.

Concluding this paragraph, one has to say that the a priori most disturbing contrast situation for layers on silicon within SEAM micrographs can be understood without difficulties in terms of the thermo-elastic theory.

Grain Boundaries

The contrast of a grain boundary in polycrystalline silicon can be understood by thermo-elastic origin, too. Influence of the thermal diffusion length becomes evident qualitatively by the micrographs of Fig. 18. With increasing modulation frequency, the structure is imaged clearer and clearer. The secondary electron image does not show any contrast in this case. Quantitative evaluation of the contrast profiles yields a $1/\sqrt{f}$-dependence (Fig. 19) of the imaged structure width which is conversely a direct measure of the frequency dependence of λ_{th}. The result of Fig. 19 is in agreement with results already obtained for grain boundaries in metals [1]. Therefore one can conclude that imaging of grain boundaries by SEAM is possible due to the mechanical discontinuity of the boundary and that semiconducting properties should be unimportant in this case.

Doping Contrast

When discussing the contrast of selectively doped regions, such as ion implantations, one has to be aware of the fact that the contrast associated with the implantation itself may be overlayed or falsified by the existence of metallizations or other coatings due to contrasts as discussed in the paragraph on "Metallization Layers". This shall be demonstrated by Fig. 20 in which a chip is imaged both in the SEAM magnitude mode and by the secondary electrons. As it still contains all oxide layers and metallizations, the contrast is dominated by these. In the middle of the micrograph, there are two double stripes located between the square metallizations. The upper one which appears bright in the SEAM image is a 0.5 µm deep phosphor implantation beneath an oxide layer. The lower one which is visible in the secondary electron image appears black in the SEAM image and is only vaguely visible there. It consists of polycrystalline silicon. After etching this chip section all the coatings and the polycrystalline silicon were taken away, resulting in a completely new contrast situation as visible in Fig. 21. The polycrystalline silicon is not visible any longer, as it was etched away, the contrast of the ion implanted stripes inverted from bright to dark.

In the following, all specimens were etched to be free of any coating to ensure that the discussion of doping contrast is not impaired by the influence of these layers. The

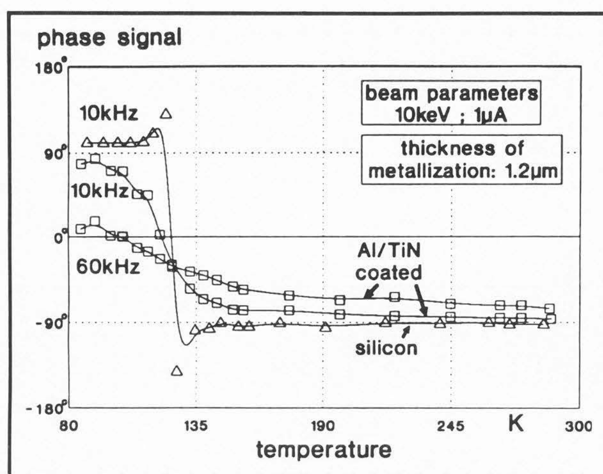

Figure 16. Electron acoustic phase signal of partially metallized silicon.

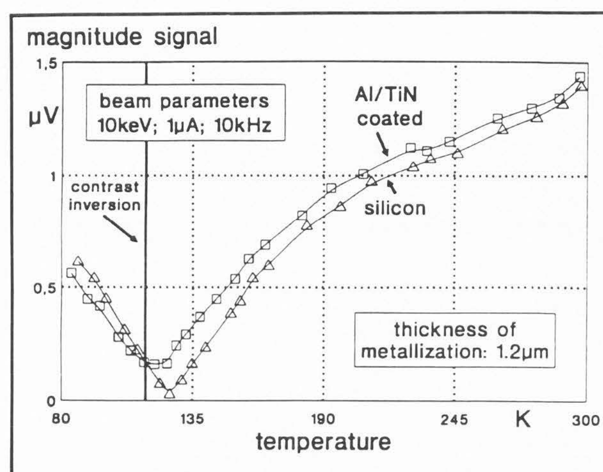

Figure 17. Electron acoustic magnitude signal of partially metallized silicon.

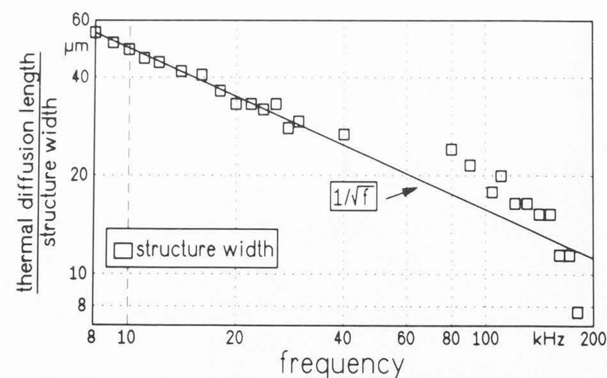

Figure 19. Frequency dependence of thermal diffusion length and structure width.

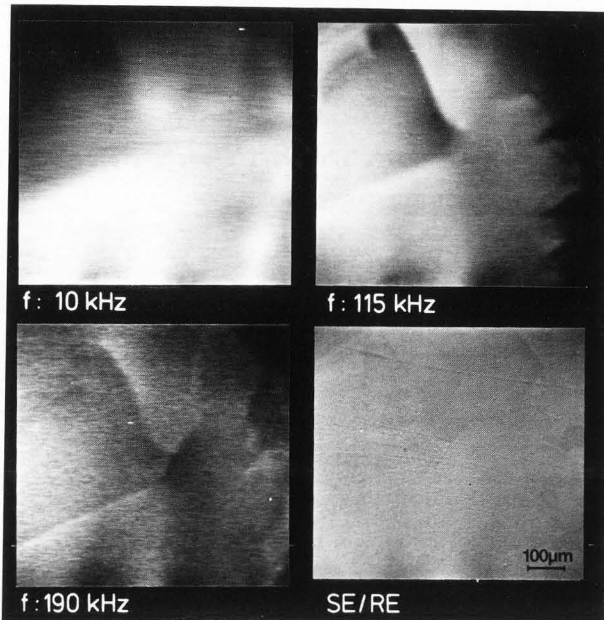

Figure 18. Micrographs of grain boundaries in polycrystalline silicon at different chopping frequencies.

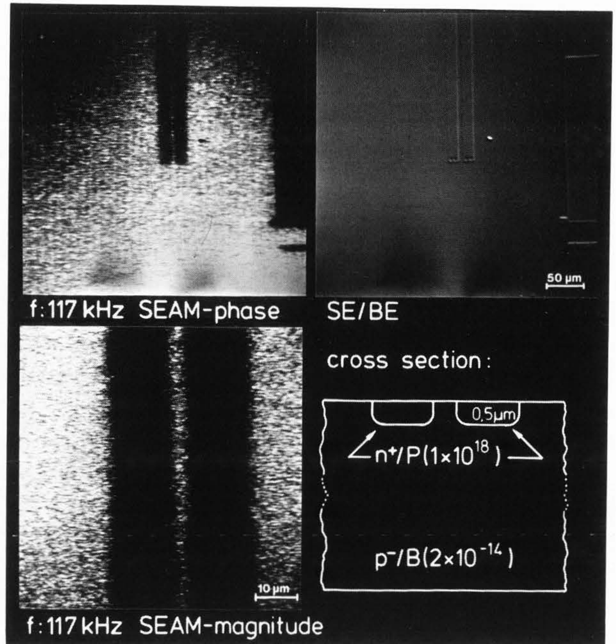

Figure 21. SEAM micrographs of selectively doped silicon.

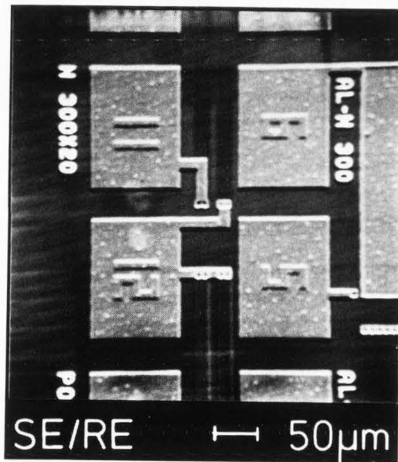

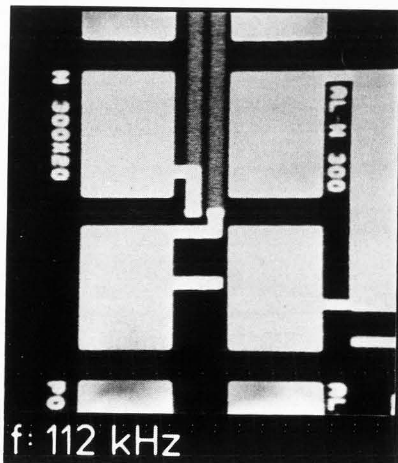

SE/RE, SE/BE: Secondary and reflected (backscattered) electrons.

Figure 20. Comparison of an electron acoustic and a secondary electron image.

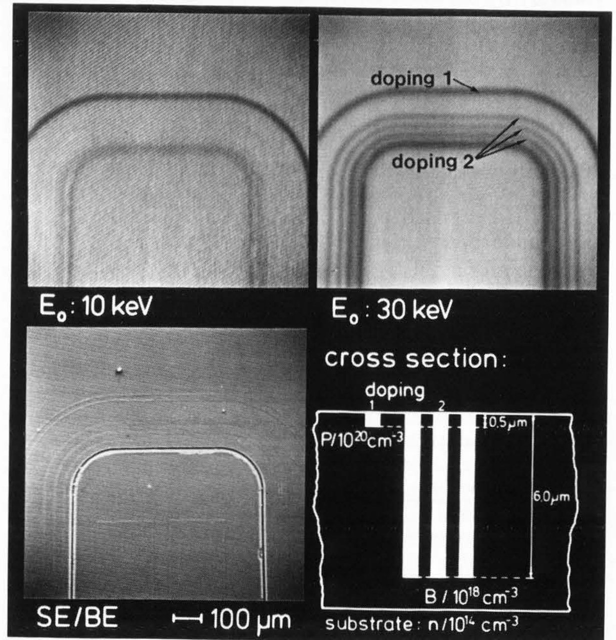

Figure 23. SEAM micrographs of selectively doped silicon.

principal thermo-elastic origin of doping contrast could be proven by both frequency and temperature dependent measurements [5], as the magnitude contrast follows the equations:

$$K(f) = s \cdot f^{3/2} + 1$$

as already shown for metallization layers,

and

$$K(T) = \left[\frac{\lambda_{th}(300\ K)}{\lambda_{th}(T)} \right]^3 \cdot s + 1$$

However, the doping contrast can only be imaged, if the primary electron dissipation volume overlaps the concentration gradient at the bottom of the implantation [5]. It should be mentioned in this context that differently, but homogeneously doped wafers do not exhibit any SEAM contrast [4]. This additional influence of the primary energy dissipation volume is not explainable by thermo-elastic theory. Furthermore, it is associated with an apparent independency of the spatial resolution of the thermal diffusion length and, by this, of modulation frequency and temperature. As the latter statement could be proven by a large series of experiments, one must conclude that the energy dissipation volume is equivalent to the information volume. This is shown for the double stripe of Fig. 21 in the linescans of Fig. 22 taken across this structure. Though the signal level rises with frequency due to a reduced λ_{th}, the spatial resolution remains unchanged and does not obey a $1/\sqrt{f}$-law.

Due to these results, the authors have developed a contrast model by taking into account combined action of thermo-elastic and electronic properties [5]. Although the signal origin is thermo-elastic, it is modified by the doping - or better - carrier concentration. In this sense, the contrasts gained are both dependent on the primary energy dissipation volume and, by this, on the penetration depth of the electron beam as well as on the primary beam current, as these quantities modify the local carrier concentration via excess carrier generation. In Fig. 23 one can see that a structure vanishes, if the electron beam does not overlap the bottom of it. The 10 keV electrons cannot reach down to the bottom of the 6 µm deeply implanted region causing an invisibility of doping 2 (as defined schematically in Fig. 23).

The dependence of the phase contrast on the primary electron beam current is plotted in Fig. 24 for the two types of doping within Fig. 23. For the 0.5 µm deep doping, similar contrast behaviour arises for 7 keV and 30 keV, for the 6 µm deep doping, a contrast maximum at about 250 nA beam current becomes visible. These two effects can again be understood in a thermo-elastic model in which, however, the thermo-elastic material parameters are modified by the electron beam in simultaneous dependence on the local doping or carrier concentration. In this manner, a contrast may only be gained, if the beam current is large enough to change the thermo-elastic properties from an undisturbed to a disturbed status. This should lead to an increase of contrast with primary beam current. However, this contrast relies additionally on the difference in this disturbance due to a different doping concentration. With increasing beam current, however, the difference between substrate and ion implanted regions decays, as the increased number of excess carriers equalizes the electronic situation within these two regions. These two opposite effects lead to the following: for high beam currents the contrast should decay always; for small beam currents there should be a maximum when both contributions are counterparting each other. That this maximum is only visible for the 6 µm deep structure and not for the 0.5 µm deep one is to be explained with the extreme experimental problems involved, as the overall signal itself decays linearly when reducing the beam current [4] and as therefore a contrast relates only to a very small electrical signal.

Concluding, the experimental results document the importance of the interaction of the primary electrons within their energy dissipation volume with semiconductor properties as the origin for the doping contrast. Nevertheless the actual height of the contrasts gained is still to be understood in terms of the thermo-elastic model.

Conclusions

With this paper, combined with previous work of the authors [4-6], a complete understanding of signal generation and contrast mechanisms within SEAM micrographs could be obtained. Based on these results it seems now to be possi-

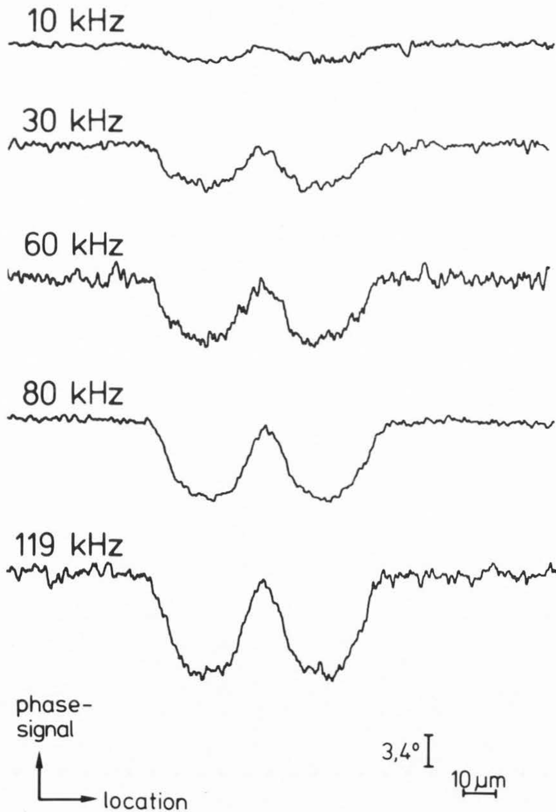

Figure 22. Lateral resolution of the doping contrast.

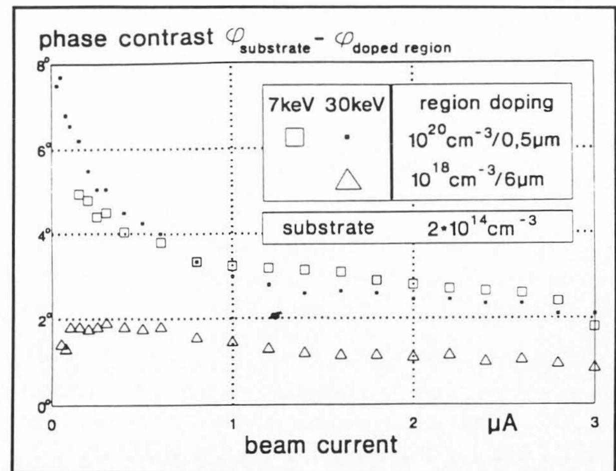

Figure 24. Doping contrast of electron acoustic phase signal versus beam current.

ble to apply SEAM quantitatively to the examination of silicon materials and devices. Applications in this sense may be local determination of thermal parameters like λ_{th} or local specimen temperature; finally, non-destructive evaluation of the three-dimensional structure of selective dopings with a lateral and axial spatial resolution which is solely determined by the energy dissipation function of the primary electrons.

A drawback of the technique is at present the need for fairly high beam currents to carry out quantitative experiments. If it is possible to overcome this problem by improved transducing and amplifying techniques, the method might be a relevant inspection tool within silicon technology, the possible spatial resolution to be in the range of 0.1 μm.

Acknowledgements

The authors like to thank first of all Prof. E. Kubalek in whose laboratory this work was carried out. Financial support was given by the Deutsche Forschungsgemeinschaft. Various institutions helped in preparing the samples: the Fraunhofer Institute Duisburg (Prof. Zimmer), the department for semiconductor technology of Duisburg University (Prof. Tegude), and Dr. Weigel from Wacker Chemitronic.

References

1. L.J.Balk, D.G.Davies, N.Kultscher: The Dependence of Scanning Electron Acoustic Microscopy (SEAM) Imaging of Chopping and Detection Frequency for Metal Samples, phys. stat. sol. (a) 82 (1984) 23 - 33.

2. E.Brandis, A.Rosencwaig: Thermal-Wave Microscopy with Electron Beams, Appl. Phys. Lett. 37 (1980) 98 - 100.

3. G.S.Cargill III: Electron-Acoustic Microscopy, Scanned Image Microscopy, ed. E.A.Ash, Academic Press, London (1980) 319 - 330.

4. M.Domnik, L.J.Balk: Evaluation of the Temperature Dependence of Electron Acoustic Signals in Silicon by Use of a Capacitive Transducer, Proceedings of the 6th International Topical Meeting "Photoacoustic and Photothermal Phenomena II", Springer Series in Optical Sciences 62 (1990) 428 - 430.

5. M.Domnik, L.J.Balk: Signal Generation and Contrast Mechanisms in Electron and Photo Acoustic Imaging of Differently Doped Silicon, Proceedings of the 19th International Symposium on Acoustical Imaging, Plenum Publishing (1992) 755 - 759.

6. M.Domnik, L.J.Balk: Capacitive Transducers for Scanning Electron Acoustic Microscopy (SEAM), Proceedings of the 19th International Symposium on Acoustical Imaging, Plenum Publishing (1992) 773 - 778.

7. G.Rousset, F.Lepoutre, L. Bertrand: Influence of thermoelastic bending on photoacoustic experiments related to measurements of thermal diffusivity of metals, J. Appl. Phys. 54 (1983) 2383 - 2391.

8. R.G.Stearns, G.S.Kino: Effect of electronic strain on photoacoustic generation in silicon, Appl. Phys. Lett. 47 (1985) 1048 - 1050.

9. R.M.White: Generation of Elastic Waves by Transient Surface Heating, J. Appl. Phys. 34 (1963) 3559 - 3567.

Discussion with Reviewers

S. Bahadur: You have mentioned the preference of using a capacitive transducer over a piezoelectric transducer for a variety of reasons in the thermoelastic generation and detection technique from the Si samples. Have you actually used a piezoelectric transducer for a comparison? If so, what material was it and how were the spurious resonances of the piezoelectric transducer eliminated? Additionally, what kind of resonances for example, flexural, extensional, thickness- or face-shear etc. were generally noticed?

Authors: In this work a direct comparison between a piezoelectric and a capacitive transducer is made. The results of Fig. 2 are obtained within the compartment as shown in Fig. 1 both for capacitive transduction and for the use of a PZT based detector. A further qualitative comparison is presented by the micrographs of Fig. 3. Within these measurements flexural vibration modes were detected (compare additionally Fig. 6 of ref. [6]). No special attempts were undertaken for suppression of these modes.

S. Bahadur: You have generally used beam parameters as 10 keV and 1 μA for investigating electron acoustic signal from metallized surfaces. Perhaps, a higher beam current would be better choice for studying contrast of selectively doped regions. Your comments on this suggestion are invited.

Authors: As can be seen in Fig. 24, for instance, a reduction of the primary electron beam current should be accompanied by an increase in SEAM contrast. This certainly would result in a smaller influence of the beam on the specimen. Unfortunately, however, the detectable SEAM signal may be too small to be detected for small beam currents.

J.F. Bresse: How do you correct for temperature changes, the capacity and the SEAM signal?

Authors: Variations of temperatures consequently lead to changed dimensions of the detector capacity. This could be determined during the experiment via a capacitance bridge enabling a corresponding calibration of the results obtained.

J.F. Bresse: From literature data ($k = 1.5\ W(cm \cdot s \cdot K)^{-1}$, $C = 0{,}711\ J/g$, $D_{th} = 0{,}91\ cm^2/s$), the value of the thermal diffusion length in silicon is at 10 kHz = 54 μm, at 1kHz = 170 μm. How do you explain the discrepancy between the expected value at T = 100 K, perhaps a factor 3 greater, and the sample thickness, for fig. 2 and fig. 7.

Authors: First of all, it must be emphasized that the value of 54 μm for λ_{th} at 10 kHz has been determined with good precision by our measurements for the case of room temperature (compare Fig. 19).

Measurements at 1 kHz were not carried out within this work.

To understand why λ_{th} differs at 100 K temperature from the expected value, one must consider various topics: λ_{th} is an artificial quantity identifying a 1/e-decay. This does not mean, however, that a temperature influence may not be measured before the amount of λ_{th} reaches the specimen thickness. This becomes evident in Fig. 2.

In a similar sense a deviation between the results for 10 kHz and 55 kHz does not start abruptly with λ_{th} = d. According to Rousset et al. [7] a gradual change from a 1/f-dependence to a frequency independent behaviour occurs already before λ_{th} reaches d.

Finally one should mention the enormous difficulties in getting reliable material data. Especially for thermal capacity and conductivity strongly differing values are reported. Thus using these certainly higher λ_{th}-values could be calcu-

lated. This problem is especially important for the temperature range in which λ_{th} depends strongly on T. We have tried to use those material data which are most recommended.

J.F. Bresse: In the section "Quantitative Determination of the Thermal Diffusion Constant", you mention the 3D effect for the theory. But theoretical calculations have given the same dependence with the thermal and the elastic parameters. (see for example, J.L. Holstein, J. Appl.Phys. 58, 2008(1985)). Can you explain?

Authors: In principle there are two 3D effects. One is combined with the dependence of the doping contrast on primary electron energy. The second one is related to the influence of λ_{th} on the results obtained for layered structures. Considering the latter case one has to mention the following: The work by J.L. Holstein treats the sample as homogeneous and as extending into infinity. Therefore statements concerning the influence of layered structures cannot be obtained with Holstein's theory. In this sense a first approximation of the heated volume by $\lambda_{th} \cdot \lambda_{th} \cdot \lambda_{th}$ is quite usual like the use of the quantity λ_{th} itself (already before the publication of Holstein's theory).

J.F. Bresse: In the section "On the Influence of Specimen Preparation", your experiment does not mention the doping level of the silicon. In the experiments of Stearns and Kino, the silicon was low doped and the excess carriers density is important due to the long lifetime. Can you comment?

Authors: To achieve a maximum life time for electron-hole-pairs, as was the case in the experiments of Stearns and Kino, a wafer material was chosen with high resistivity (3750 - 6250 Ωcm).

G.S. Cargill III: You conclude "that imaging of grain boundaries by SEAM is possible due to the mechanical discontinuity of the boundary . . ." Do you mean a mechanical discontinuity in the sense that the boundary interrupts the heat flow, or in the sense that the boundary interrupts the propagation of the acoustic (displacement) wave?

Authors: There is no noticeable influence of the grain boundary onto the acoustic wave. According to the large acoustic wavelength, as can be seen by the according vibrational mode patterns, such an influence should not be expected (compare Fig. 6 of ref. [6]).

G.S. Cargill III: Can you give a simple physical explanation of your observation in Fig. 23 "that a (doping related) structure vanishes, if the electron beam does not overlap the bottom of it"?

Authors: With sufficiently low primary electron energies the energy dissipation volume is transferred from the implanted region into the surrounding substrate. In both extremes it changes its position from one homogeneous material to another. According to these homogeneities no contrast can be gained, as the formally existing difference is counterparted (compare ref. [5]).

J.C. Murphy: The use of capacitive detection in SEAM is interesting. However, some aspects of the comparison between capacitive and piezoelectric detection are unclear. For example, given that the resonances seen in piezo-detection are some composite of sample, substrate and detector mechanical properties as noted in the paper, should the capacitive and piezo-detection methods exhibit substantial differences due to the noncontact detection for the capacitive method? This is not discussed in the text and does not appear to be seen in the experiments.

Authors: Both quantitative results for the temperature dependences of SEAM magnitude and phase and the qualitative comparisons within the micrographs have shown in detail the equivalence of piezoelectric and capacitive transducers. The only exception is given for a thermally thin sample, in which a signal intrusion occurs due to a direct heating of the piezoelectric transducer, as discussed within this paper. The necessary mechanical coupling of the sample to the piezoelectric transducer influences the vibrations of the sample unavoidably causing a somewhat chaotic frequency behaviour with a large number of more or less pronounced resonances (compare Fig. 7 in ref. [6]). Although these effects alter the detectable signal level, the signal's origin is still the same for both detection schemes. Therefore, with the only exception as mentioned above, the results obtained are identical for both transducers.

J.C. Murphy: The paper presents itself as addressing the contrast mechanisms for SEAM. It does not contain any discussion of acoustic contrast at mechanical features, however. It also does not discuss the presence or absence of carrier recombination effects despite their presence in a wide range of related thermal imaging experiments in silicon. These mechanisms are nowhere acknowledged in the text.

Authors: With Figs. 18 and 19 the influence of a mechanical discontinuity, i.e. a mechanical feature, could be identified as a contrast origin.

The influence of different recombination properties of electron-hole-pairs has been treated in detail. Within the experiment related to Fig. 12 a high resistivity material was used which was differently surface treated. A polished and a damaged surface were compared. In spite of different recombination properties at the surface no significant signal change could be measured. Similarly all results within the frequency dependences (Figs. 9 - 11 and Figs. 1 - 3 of ref. [5]) have not at all shown any additional time-dependent contribution as should be assumed for a significant recombination contribution. As, furthermore, identical results were obtained both for metals and silicon, recombination effects can be excluded for the signal generation. Therefore further discussion of these effects has been omitted in the following.

This paper and the authors' reference [5] are dealing in detail with a most prominent example of thermal imaging, the doping contrast within semiconductors. Both papers could prove unequivocally that the theory by Rosencwaig & White does not deliver a correct explanation. Furthermore, the doping contrast as arising from the extension of the energy dissipation volume with relation to the doping depth cannot be treated as thermal imaging only.

J.C. Murphy: In the section "On the Influence of Specimen Preparation", the authors address the issue of surface preparation. This issue is not limited to just the issue of photostriction. In the event that the surface recombination velocity is low, then photogenerated carriers are expected to diffuse from the surface and to recombine inside the material as shown by Fournier et al. This adds a second thermal term to the generation process which has a different depth dependence, including a different result for the response as a function of sample thickness than that considered by the authors.

Authors: A second thermal term as shown by Fournier et al. could not be detected in any of our experiments. The changes of the SEAM signal with specimen thickness are not due to recombination properties and can be detected for metals in the same identical manner (compare the theory by Rousset et al. in ref. [7]).

J.C. Murphy: Regarding the experimental studies themselves and the dependence on sample thickness and temperature, are the measurements reported carried out with the electron and/or laser beam on epicenter relative to the center of the detector? This should be important when discussing the effective thermal thickness of thin samples at any temperature.

Authors: For the quantitative measurements the sample was always excited in its epicenter. The distance to the detector cap was always larger than the specimen thickness. Thus the addressed problem can be neglected.

J.C. Murphy: Referring to the section "Doping Contrast", it may be that the beam voltage contrast is associated with the beam interaction volume overlapping the bottom of the dopant region. However, there are other views of such contrast (see our review paper in IEEE UFFC-1986) and this paper does not demonstrate the claimed response with depth. For example, what evidence is there that the e-beam current modifies the material parameters of the specimen at the low currents present in the experiment? There is certainly a voltage dependence but what evidence is there for a current dependence?

Authors: First some general comments to the paper by Murphy et al. (IEEE Trans. Ultrasonics, Ferroelectrics, and Frequency Control, vol. UFFC-33 No. 5 (1986), 529-541): The beam specimen contrast as discussed in the reference mentioned has no relation to the one as discussed in the present paper. A contrast is assumed there to originate from an enlarged primary electron energy and a subsequent change of electron energy dissipation (compare Fig. 5 of Murphy et al. and the according comment of page 533). The result as reported is mainly a proof of the well-known assumption that the final spatial resolution is a sum of the extension of the energy dissipation volume and of the thermal diffusion length. As λ_{th} is smaller than the penetration depth of 30 keV primary electrons (for a frequency of assumed 400 kHz) the effects within Fig. 5 of Murphy et al. are to be expected.

Why can this example not give reliable information on the other hand? First of all, an undefined IC was tested at an undefined position. Further, the IC still was covered with all surface layers. As could be shown by the authors' work in detail, contrasts may become very ambiguous, if these layers are not etched away.

The decreasing spatial resolution with frequency is contrary to our results and may lead to the assumption that some other feature has been detected, for instance a mechanical defect, and not a precisely defined implantation.

Murphy's contrast explanation presumes the energy dissipation volume to be completely within different material region. However, the doping contrast as reported in the present paper necessitates an overlap of the dissipation volume in two different material regions (implanted region and substrate).

To answer the last question: The material parameters are changed by the number of high energetic electrons and thus indirectly by the beam current. The effect of a changed material parameter can be concluded from the combined action of thermoelastic properties and the influence of the energy dissipation volume. The detected influence of λ_{th} identifies this material parameter as a thermo-elastic quantity. The constancy of the spatial resolution with frequency shows the influence of the energy dissipation. As the results can be obtained in a reversible manner, a possible specimen damage can be excluded.

S. Myhajlenko: The authors detect the fundamental modulation frequency (f) of the SEAM signal via a lock-in technique. Have the authors used the 2nd harmonic (2f) which is equivalent of electronic differentiation of the f mode signal in imaging experiments? This signal may contain additional 'morphological' information?

Authors: No, this paper was solely restricted to detection at f, one reason being that no significant 2f-signal could be picked up within the experiments.

S. Myhajlenko: Would the authors expect stresses in thin layers to influence the electron acoustic spectral response, for example, in implanted regions such as those depicted in Figure 23?

Authors: Yes, it may be possible. However, there should be three different contributions: the 1/f-thermo-elastic behaviour, resonance properties as mentioned in the text, and finally stress at the interfaces as the thermo-elastic information volume extends across them (compare [5]).